

Acoustic and relaxation processes in supercooled o-ter-phenyl by optical-heterodyne transient grating experiment

R. Torre^{1,2}, A. Taschin^{1,3}, M. Sampoli^{1,4}.

¹ *INFM, Unità di Firenze, largo E.Fermi 2, I-50125, Firenze, Italy*

² *LENS, Università di Firenze, largo E.Fermi 2, I-50125, Firenze, Italy*

³ *Dip. di Fisica, Università di Firenze, largo E.Fermi 2, I-50125, Firenze, Italy.*

⁴ *Dip. di Energetica, Università di Firenze, via S.Marta, Firenze, Italy.*

(6/1/2001)

Abstract

The dynamics of the fragile glass-forming o-ter-phenyl is investigated by time-resolved transient grating experiment with an heterodyne detection technique in a wide temperature range. We investigated the dynamics processes of this glass-former over more then 6 decades in time with an excellent signal/noise. Acoustic, structural and thermal relaxations have been clearly identify and measured in a time-frequency window not covered by previous spectroscopic investigations. A detailed comparison with the density response function, calculated on the basis of generalized hydrodynamics model, has been worked out.

I. INTRODUCTION

Supercooled liquids and glasses have been the subject, in these last years, of an extensive theoretical and experimental study [1,2]. One of most important features of these materials is the wide range of times scales over which relaxations occur at fixed and mostly changing temperature. The relaxation times can span over many decades (up to 13 decades) when temperature is varied from the melting to glass transition temperature. Indeed these relaxation processes have a complex nature that, despite the recent research efforts, remain unclear in many aspects. Among the others, a fundamental issue is the interplay of different dynamical variables present in these materials. So that the rotational dynamics and its coupling with the translational variables are under an intense experimental investigation [3–5]. Even when a single variable (e.g. density) is studied, many processes are involved in the glass dynamics (like for example the acoustic, structural and thermal relaxation) and they are usually characterized by different time scales. From the experimental point of view, it is of fundamental importance to measure the investigated variables over the full temporal or frequency range. Often this is accomplished hardly by the combination of several techniques (e.g. Light Scattering, Photon Correlation Spectroscopy, etc.) since, even if the same experimental observable is tested, the very wide frequency or time domain with possible not overlapping range, preserves a reliable analysis of the data.

The transient grating technique (TG) is well know to give a unique experimental insight in the dynamics of fluid and glassy material [6]. Recently this technique has been applied to the study of dynamics of supercooled liquids [7]. Using a CW beam probe it has been covered a very wide temporal range, from n sec to m sec, in a single experiment giving an unique access to the glass dynamics.

In this paper we present a study of relaxation dynamics of the fragile glass-former ortho-ter-phenyl (OTP) by optical Heterodyne Detected Transient Grating (HD-TG) experiment. Acoustic, thermal and structural relaxations are investigated in wide temperature range, from above the melting down to the glass-transition. This HD-TG experiment produces data

with an extremely high signal/noise ratio and allows to detect and measure signals even of very low level. We present a study of the complex relaxation pattern of the density in a prototype of the fragile glass-formers, OTP, and we put in evidence some new features of the slow thermal relaxation that can not be properly accounted for by the standard hydrodynamic model.

The paper begins (sec. II) with a brief description of the transient grating experiment and in particular underlines the improvements that can be obtained by using an optical heterodyne detection. In sec. III the theoretical background needed for data analysis and interpretation is given. A detailed description of the OTP measurements is written in sec. IV and in sec. V we present all data and their analysis. The last sec. VI is devoted to discussions and conclusions.

II. HETERODYNE TRANSIENT GRATING EXPERIMENT

In a transient grating (TG) experiment two high power laser pulses interfere inside the sample and produce a spatially periodic variation of the index of refraction [6,8]. A third laser beam, typically of different wavelength, is acting as a probe by impinging on the induced grating at the Bragg angle and producing a diffracted beam, spatially separated by the pump pulses and probe beam, see fig.1. This diffracted beam is the signal measured in a TG experiment and yields the dynamic information from the relaxing TG. The spatial modulation in the TG defines a wave-vector q characterizing the diffracted beam and hence the signal. The q wave-vector is:

$$q = \frac{4\pi \sin\left(\frac{\theta_e}{2}\right)}{\lambda_e} \quad (1)$$

where λ_e and θ_e are the wavelength and the incidence angle of the excitation laser pulses. When, as usual, the homodyne scheme is used to detect the diffracted beam, the diffraction efficiency results to be proportional to the square of the refraction index variation so that small variations produce even smaller signal. A considerable improvement can be obtained

by using an optical heterodyne detection (HD). Indeed in our HD-TG experiment, the measured signal is given by:

$$S(q, t) \propto \langle |E_d(q, t)|^2 \rangle + \langle |E_l|^2 \rangle + 2 \langle |E_d(q, t)| \rangle \langle |E_l| \rangle \cos \Delta\varphi \quad (2)$$

where E_d is the electric field diffracted by the TG, E_l is the local beating field and $\Delta\varphi$ is the phase difference between the E_d and E_l , see fig.1, $\langle \cdot \rangle$ represent the time-averaging over the optical period, e.g. $\langle |E_d(q, t)| \rangle$ is the amplitude of the oscillating diffracted electric field. The first, second and third terms in the r.h.s. of eq. 2, are the homodyne ($\langle |E_d|^2 \rangle$), local field ($\langle |E_l|^2 \rangle$), and heterodyne contributions ($2 \langle |E_d(q, t)| \rangle \langle |E_l| \rangle \cos \Delta\varphi$) respectively. Normally, the local field is kept constant and much higher than the diffracted one, so that the homodyne contribution becomes negligible and the time variation of the signal is dominated by the heterodyne term. In addition, this last term can be experimentally isolated by subtracting two recorded signals with different phases, and in particular the first one, S_+ , with $\Delta\varphi_+ = 2n\pi$ and the second, S_- , with $\Delta\varphi_- = (2n+1)\pi$ (n integer). It is evident that:

$$S_{HD}(q, t) = [S_+ - S_-] \propto \langle |E_d(q, t)| \rangle \langle |E_l| \rangle \quad (3)$$

We have two major advantages in using the heterodyne instead of homodyne detection. First, we can improve substantially the signal to noise ratio in the all time window, both because of the high level of the local field and because of discarding spurious signals which are not reversed by a π phase shift of the local field. Second, the sensitivity at long times when the TG is vanishing, is enhanced enormously since the recorded signal is proportional to $\langle |E_d| \rangle$ instead of being proportional to its square. In the studies of materials with a weak scattering efficiency and complex response, these features turns out to be of basic importance. Nevertheless, the effective realization of such a detection is quite difficult at optical frequencies. Indeed to get an interferometric phase stability between the diffracted and the local field is not a simply experimental task, and so only few HD-TG experiments have been realized up to now [6]. Recently the introduction of phase gratings in the optical setup of TG experiments has reduced considerably the difficulties of using a heterodyne detection [9,10]. The details of this new setup will be described in Sec. IV A.

Formally, in the limit of linear response theory the average diffracted field is proportional to the specific response function of the material convoluted with the excitation force produced by the laser excitation [8]. Assuming the impulsive limit in time (i.e. the excitation time much shorter than the observable characteristic times) and in wave-vector (i.e. the excitation spot size much larger than the material wavelength scale) we have:

$$S_{HD}(q, t) \propto \langle |E_d(q, t)| \rangle \propto R(q, t). \quad (4)$$

The response function, $R(q, t)$, describes how the exciting pulses are effective in producing a TG, i.e a periodic variation of the optical properties out of equilibrium, and how this variation is relaxing toward equilibrium. If the duration of exciting pulses has to be taken into account, i.e. if some characteristic times in the responses can not be considered long enough with respect to the pulse duration, the total response has to be calculated from the appropriate convolution.

The response function has a tensorial nature, R_{ijkl} , where the different component are selected through the excitation, probing and detection directions of polarizations. In the present experiment all these polarizations are taken vertical, i.e. normal to the scattering plane, (see Sec.IV A for details) and then we are dealing with a single tensorial component of the response function, R_{VVVV} .

The interaction of the excitation laser field with the material is responsible of generating the TG and defining the response function. Depending on the nature of this interaction, the excitation laser pulses can produce a modulation of the real part of the refraction index (i.e. a birefringence and/or a phase grating), and/or a modulation of the imaginary part (i.e a dichroic and/or absorption grating). Which grating is excited and how its dynamics reflects the material properties is a complex problem that can be solved only under certain conditions and approximations.

As well as other molecules of glass forming materials investigated by TG [7], our OTP molecule has no electronic absorption band at the pump and probe wavelengths. However the strong near infrared pulses are absorbed weakly by overtones and/or combinations of

vibrational bands. Typically, these vibrational excitations thermalize in few picoseconds. According to Nelson and co-worker [7] the induced TG can be described approximately as a pure phase grating generated by two different mechanisms of laser-matter interaction: a temperature grating produced by the field induced heating and a pressure electrostrictive grating due to the field gradient. In this approach, no birefringence effects are taken in account, such as a modification of the molecular polarizability orientation due to field effects (optical Kerr effect) or to a molecular alignment induced by roto-translation coupling. For materials composed by molecules of nearly isotropic shape and without strong anisotropic interactions, such as the OTP under the present investigation, the total response should be considered mainly driven by the density. We verified experimentally this hypothesis measuring the S_{HHVV} signal (with the probe and detection polarizations, HH , perpendicular to the excitation one, VV) and comparing that with the S_{VVVV} signal: no meaningful difference has been detected for any temperature in OTP. So in this molecule no relevant birefringence effects are present confirming that the response function can be mainly described by the density dynamics. Viceversa strong difference has been detected in a other glass-former, (e.g. *m*-toluidine and salol), showing that the response function of glass-formers made of anisotropic molecules must include birefringence and roto-translational coupling effects [4].

By taking into account the two mechanism above mentioned, the measured signal is proportional to the q -component of the density variations and is composed of three different contributions: roughly speaking, two coming from the heating and one from the electrostriction. i) The part of the solid like or fast liquid response of the sample to the sudden heat flux, launches a sound wave of frequency $\omega_A = c_A q$ around the mean density at the new local temperature. The sound wave is damped with the acoustic time constant τ_A and then the local temperature relaxes with a time constant τ_H due to the thermal diffusivity. Therefore this contribution can be written as: $\rho_q^{(h,s)} \propto [1 - \exp(-t/\tau_A) \cos(\omega_A t)] \exp(-t/\tau_H)$. ii) The part of viscous liquid response to the heat flux produces a slow density variation which grows up with a time constant τ_R and vanishes again with the thermal diffusivity constant, i.e. $\rho_q^{(h,r)} \propto [1 - \exp(-t/\tau_R)] \exp(-t/\tau_H)$.

iii) The sudden density momentum change due to the electrostriction launches a sound wave of the same frequency $\omega_A = c_A q$ around the normal density which is damped always with the same acoustic time constant, i.e. $\rho_q^{(e)} \propto \exp(-t/\tau_A) \sin(\omega_A t)$.

Intuitively the sum of these contributions will be the measured signal. Obviously there can be interactions among the contributions if the time constants are not well separated, indeed this separation has been supposed implicitly in the previous derivation. Further, the viscous response in supercooled liquids is made of a distribution of time constants instead of single time. In the next section we derive the forced density fluctuations from the hydrodynamic equations and important relations among the parameters we have introduced.

III. THEORETICAL BACKGROUND

The generalized hydrodynamics equations have been often used to describe the frequency resolved light scattering experiments [11]. They express the conservation law the dynamics of the fluid is subjected to: the conservation of mass, momentum and energy. As usual, we neglect the effects of rotational dynamics, as already discussed and we use the linearized form of the hydrodynamic equations (small fluctuation out of equilibrium) [12]. Since we are interested to the q-component of the density fluctuations, we write directly the Fourier-Laplace transform (FLT) of the continuity, Navier-Stokes, and energy equations. They read

$$s \widetilde{\delta\rho_q}(s) + i q \widetilde{J_{q\parallel}}(s) = \delta\rho_q(0)$$

$$[s + \phi_L(s) q^2] \widetilde{J_{q\parallel}}(s) + i (qc_o^2/\gamma) [\widetilde{\delta\rho_q}(s) + \alpha \rho_o \widetilde{\delta T_q}(s)] = J_{q\parallel}(0)$$

$$(s + \gamma\chi q^2) \rho_o \widetilde{\delta T_q}(s) + i [q(\gamma - 1)/\alpha] \widetilde{J_{q\parallel}}(s) \delta\rho_q(s) + i q J_{q\parallel}(s) = \rho_o \delta T_q(0)$$

where $\widetilde{\delta x_q}(s)$ stand for the FLT of the fluctuating quantity $\delta x(\mathbf{r}, t)$, i.e.

$$\widetilde{\delta x_q}(s) = \int_0^\infty dt \exp(-st) \delta x_q(t) = \int_0^\infty dt \exp(-st) \int_{-\infty}^{+\infty} d^3r \exp(i\mathbf{q} \cdot \mathbf{r}) \delta x(\mathbf{r}, t)$$

and ρ_o is the equilibrium mass density, $J_{q\parallel}$ the component parallel to \mathbf{q} of the mass current density, δT_q the fluctuating temperature, c_o the adiabatic zero frequency sound velocity, $\gamma = C_p/C_v$ the ratio of the specific heats, $\alpha = -(\partial\rho/\partial T)_p/\rho$ the coefficient of thermal expansion, $\chi = k(\rho_o C_p)^{-1}$ the thermal diffusivity, and $\rho_o \phi_L$ the longitudinal kinematic viscosity.

Following Nelson [7,13], we can solve formally the previous equations with the starting conditions $\delta\rho_q(0) = 0$, $J_{q\parallel}(0) = i q F$, and $\rho_o \delta T_q(0) = Q/C_v$ and we obtain that the HD signal can be written in the Nelson's notation as:

$$S_{HD}(q, t) \propto R_\rho(q, t) = -F G_{\rho\rho}(q, t) + Q G_{\rho T}(q, t) \quad (5)$$

where $G_{\rho\rho}(q, t)$ is the response to the electrostriction (also called Impulsive Stimulated Brilluoin Scattering, ISBS) , and $G_{\rho T}(q, t)$ to the absorption (also called Impulsive Stimulated Thermal Scattering, ISTS) [6,7]. F and Q are two constants that define, respectively, the magnitude of the electrostriction and heat flux in the limit of infinitely short pump laser pulses.

In order to calculate the density response function, we have to know all the coefficients and in particular the time (or frequency) dependence of the kinematic viscosity ϕ_L . Only for particular form of ϕ_L it is possible to obtain analytical expressions for $G_{\rho\rho}(q, t)$ and $G_{\rho T}(q, t)$. One of them is the very simple but useful Debye model of a viscous fluid where the kinematic viscosity (or memory function for the elastic modulus) is approximated by the sum of an instantaneous plus a exponential relaxing term: $\phi_L(q, t) = v_L \delta(t) + (c_\infty^2 - c_0^2) \exp(-t/\tau_R)$. If all the characteristic times (i.e. the period of the acoustic wave, its damping time constant, the structural relaxation time and the thermal diffusion time constant) are well separated each other , very simple equations are obtained [7,13,14]:

$$G_{\rho T}(q, t) \simeq A \left[e^{-\Gamma_H t} - e^{-\Gamma_A t} \cos(\omega_A t) \right] + B \left[e^{-\Gamma_H t} - e^{-t/\tau'_R} \right] \quad (6)$$

$$G_{\rho\rho}(q, t) \simeq C \left[e^{-\Gamma_A t} \sin(\omega_A t) \right] \quad (7)$$

where: Γ_H is the thermal damping rate ($\Gamma_H = 1/\tau_H = \chi q^2$), τ'_R the effective structural relaxation time ($\tau'_R = \left(\frac{c_A}{c_0}\right)^2 \tau_R$ being c_A the sound velocity), ω_A and $\Gamma_A = 1/\tau_A$ are the frequency and damping of acoustic longitudinal phonon, A , B , and C are constant dependent on sample and experimental setup. The importance of this treatment resides in the possibility to extract other information and to make expectations on the general behavior of the various parameters versus q and temperature. In particular we expect a maximum on the acoustic damping both versus q and T , and a gradual shift of the sound velocity from c_0 to c_∞ lowering the temperature or increasing q . We have [13]:

$$\omega_A = c_A q = \left[c_0 \sqrt{D + \sqrt{D^2 + (c_0 q \tau_R)^{-2}}} \right] q; \quad D = [c_\infty^2/c_0^2 - (c_0 q \tau_R)^{-2}]/2 \quad (8)$$

$$\frac{\Gamma_A}{q^2} = \frac{1}{2} \left\{ [v_L + \chi (\gamma - c_0^2/c_\infty^2)] + \frac{c_\infty^2 - c_0^2}{1 + \omega_A^2 \tau_R^2} \right\} \quad (9)$$

Further, always in the assumption that $\omega_A \gg \Gamma_A \gg \tau_R^{-1} \gg \Gamma_H$ and some other minor approximations [13], we can extract the Debye-Waller factor or non-ergodicity parameter $f_{q \rightarrow 0}(T)$ from A and B coefficients which in turn can be derived by fitting the experimental data with the theoretical expression:

$$f_{q \rightarrow 0}(T) = 1 - \frac{c_0^2}{c_\infty^2} = \frac{B}{A + B} \quad (10)$$

However, the Debey model for the longitudinal kinematic viscosity has severe limitations. As it has been pointed out in many experimental works, the structural relaxation around the critical temperature of the structural arrest is not reproduced by a single relaxation time but by a distribution of them; often this fact has been attributed to the rise of heterogeneities during the cooling. As a consequence, more complex models have to be used to take into account the distribution of relaxation times, e.g. by a multi-exponential or stretched exponential approach [1]. When all the relaxation times of the actual distribution are separated from the other characteristic times, the kinematic viscosity affect only the term with the B coefficient (the ii) term of the previous section) and a complex relaxation can be put directly in the response as a stretched exponential, i.e. a Kohlrausch-Williams-Watts (KWW) function [13]:

$$G_{\rho T}(q, t) \simeq A \left[e^{-\Gamma_H t} - e^{-\Gamma_A t} \cos(\omega_A t) \right] + B \left[e^{-\Gamma_H t} - e^{-(t/\tau_S)^\beta} \right] \quad (11)$$

where the 'relaxation time' τ_S and the stretching factor β are fitting parameters for the relaxation time distribution. This approximation has the advantage to keep an easy and readable form for the response function but this simplicity prevents to account for possible interactions among the different relaxing mechanisms. To compare τ_S with the relaxation times derived by other time distribution (like the Cole-Davidson in the frequency domain) or derived in single relaxation time approximation, the mean of the time distribution is calculated as $\langle \tau_S \rangle = \beta^{-1} \Gamma(\beta^{-1}) \tau_S$.

We want to remark that the presence of a stretched exponential in the $G_{\rho T}(q, t)$ can not be considered *per se* a way to introduce the mode-coupling theory in the hydrodynamic response [15].

IV. EXPERIMENTAL PROCEDURES

A. Laser system and optical set-up

The lasers and the optical set-up used to realize the HD-TG experiment are reported in fig.1. The pump infrared pulses at 1064 *nm* wavelength, are produced by a mode-locked Nd-YAG laser (Antares-Coherent) and then they are amplified by a regenerative Nd-YAG cavity (R3800-Spectra Physics) to reach 1 *mJ* at 1 *kHZ* of repetition rate with 100 *ps* of duration. The probing beam, at 532 *nm* wavelength, is produced by a diode-pumped intracavity-doubled Nd-YVO (Verdi-Coherent), this is a CW single-mode laser characterized by an excellent intensity stability with low and flat noise-intensity spectrum. The beam intensities and polarizations are controlled by two couples of half-wave plate and polarizer.

The optical set-up, shown in fig.1, uses a phase grating as a diffractive optical element (DOE): controlling the depth of the grooves and their spacing it is possible to obtain very high diffraction efficiency also better than 80% on the first two orders. Since we have to diffract both 1064 and 532 *nm* a compromise must be used. The chosen DOE (made by

Edinburgh Microoptics) gives on a single beam at first order a 12% diffraction efficiency for the 532 *nm* and 38% for the 1064 *nm*. Different spacings can be used to change the q vector. With the aid of a dichroic mirror (DM), the excitation and probing beams are sent colinearly on the DOE that produces the two excitation pulses (E_{ex}), the probing (E_{pr}) and the reference beam (E_l). These beams are collected by a first achromatic lens (AL1), cleaned by a spatial mask to block other diffracted orders and then recombined and focused by a second lens (AL2) on the sample. The local laser field is also attenuated by a neutral density filter and adjusted in phase passing through a couple of quartz slab properly etched. The excitation grating produced on the sample is mirror image of the enlightened DOE phase pattern. If AL1 and AL2 have the same focal length, the excitation grating has half the spacing of DOE [9]. This type of set-up gives automatically the Bragg condition on all the beams and produces a very stable phase locking between the probing and reference beam, a crucial parameter to realize a heterodyne detection. To properly test the acoustic damping [7] the excitation beam is focalized by a cylindrical lens (CL2) on the DOE and the produced grating on the sample is extended in the q direction (about 5 *mm*), viceversa the probing beam is focalized in a circular spot (0.5 *mm*) on the sample, through the two lens CL1 and CL2. We reduced the lasers energy on the sample to the possible lowest level to avoid undesirable thermal effects, and the CW beams has been gated in a window of about 1 *ms* every 10 *ms* by using a mechanical chopper synchronized with the excitation pulses. The mean exciting energy was 7 *mW* (35 μJ per pulse at 100 *Hz*) and the probing energy was 6 *mW*. The reference beam intensity is very low and it is experimentally adjusted, using a variable neutral filter, to be about 100 times the intensity of the diffracted signal. With these intensities the experiment is deeply inside the linear response regime and no dependence of HD-TG signal shape on the intensities of the beams can be detected. The HD-TG signal, after it has been optically filtered, is measured by the a fast avalanche photodiode with a bandwidth of 1 *GHz* (APD, Hamamatsu), amplified and recorded by a digital oscilloscope with 1 *GHz* – 4 *Gs* (LeCroy).

The OTP, from Fluka (99 %), has been purified by repeated crystallization in methanol

and dried under vacuum. The sample is kept in an aluminium cell with a teflon coating and it shows a stable supercooled phase. The cell temperature is controlled by a cryostat system (helium closed circle, Cryotip) with a platinum resistance dipped in the sample.

B. Data collection and handling

The OTP measured signal spans over many decades in time, typically up to about 1 *ms*, so we recorded the data in a pseudo-logarithmic time scale. We use a fast time window (0 – 1 μs range with a 250 *ps* time-step), an intermediate (0 – 20 μs range with a 10 *ns* time-step) and long one (0 – 1 *ms* range with a 200 *ns* time-step) and then the measurements are merged in a single data file, we did not have any problems of overlapping. Each data is an average of 5000 recording (corresponding to about 1 minute of acquisition time) and this is enough to produce an excellent signal to noise ratio. In order to get rid of the homodyne and other spurious signals, we recorded two measurements at different phases of the local field, the first signal, S_+ , with $\Delta\varphi_+ = 2n\pi$ and a second one, S_- , with $\Delta\varphi_- = 2(n+1)\pi$ (see eq.2) and then we subtracted S_- from S_+ to extract the pure HD signal, S_{HD} (see eq.3). From fig.2 where we have reported two typical S_+ and S_- signals and the extracted S_{HD} , it is clear how this procedure increase substantially the quality of data.

We measured the relaxation processes of OTP as a function of temperature for three different value of $q = 0.338, 0.630, 1.000 \mu m^{-1}$. The wave-vectors are evaluated by the geometry of the experiment and are affected by 0.8 %, 0.6 % and 0.4 % error, respectively. For each wave-vector we take data as function of temperature in a range, 243 – 373 *K*, that largely covers the liquid and supercooled region around $T_c \sim 290$, being $T_g = 244$ *K* and $T_m = 329$ *K*. In fig.3 we show in linear-log scale some representative HD-TG data on glass-forming OTP.

As is evident from fig.3, the density OTP dynamics is characterized by an acoustic phonon, a structural relaxation that appears as a rise in the signal and by the final thermal relaxation. The damping of acoustic phonon and the structural processes are strongly tem-

perature dependent. There is a temperature region where these 'modes' (acoustic phonon, structural and thermal relaxation) are characterized by separated time scales. Some physical quantities, like the sound velocity, can be directly got from HD-TG data but a complete analysis of them requires a fitting procedure.

We tested the response function defined in eq.s 7, 11 performing a non-linear least square fit on our OTP data. The fitting includes a convolution with the instrumental response (APD, amplifier and oscilloscope) especially important at small times in the acoustic oscillating part of the signal. We found this response function able to reproduce our HD-TG data on large time windows but not on the whole measured time scale, see fig.4. Indeed the very fast time scale ($0 - 2 \text{ ns}$) is fairly reproduced, even if an extreme care has been taken to include all the possible signal contributions, e.g. the instantaneous signal due to the molecular hyperpolarizability. Actually it is not surprising that an hydrodynamics approach is not appropriate on a fast time scale since it does not take into account any molecular proprieties. Again, as we will discuss later in detailed see sec.V, we found that in the long time scale ($0.1 - 1 \text{ ms}$) and in the intermediate temperature range this response function is not able to reproduce our data that show a relaxation pattern that can never be explained by the used response function, see fig.9. From our fit on OTP it is clear the presence of both the excitation mechanism: the electrostrictive effects (ISBS contribution) and the thermal effects (ISTS). We can estimate about 60% of ISBS against 40 % of ISTS for $q = 0.338 \text{ } \mu\text{m}^{-1}$ and this ratio increases when the value of the wave-vector increases. Nevertheless from the fitting the two contributions can be safely disentangled, thank the linear access to the response function. To evaluate the errors for such complex data and fitting function is not a trivial task, we used an 'a posteriori' procedure. We repeated the experiment getting for each temperature and wave-vector several HD-TG signals, then we fit all the signals producing a distribution of parameters.

V. RESULTS

We used the previously defined response function (see eq.s 5, 7, 11) to extract the information about OTP dynamics from HD-TG data. The fitting parameters are: the acoustic frequency and damping rate (ω_A and Γ_A), the structural relaxation time and stretching parameter (τ_S and β), the thermal relaxation time (τ_H) and the amplitude constants (A , B and C). In fig.5 we report the sound velocity, $c_A = \omega_A/q$, and the damping rate, Γ_A , see table I. At all the investigated temperatures and wave-vectors these two parameters are extracted with very small uncertainties, less than 1%. The sound velocity, see fig.5a), shows the typical temperature dependence of viscoelastic liquids. The velocity increases lowering the temperature and shifts from two linear dependence regime, at high temperatures the velocity almost corresponds to the adiabatic sound velocity, c_0 , while at low temperatures corresponds to the solid-like or 'infinite' frequency sound velocity, c_∞ . In the transition region, starting from a few ten of degree above T_c , there is a rapid increase of c_A toward c_∞ . At higher wave-vector the shift between the two regime appears at higher temperature. This behavior reflects the rapid variation of the structural relaxation time with the temperature. In fact at high temperatures the structural relaxation time is shorter than the phonon oscillation period, $\tau_S \ll (\omega_A)^{-1}$ and the relaxation process is coupled weakly with the sound yielding a soft damping. Again at low temperatures when $\tau_S \gg (\omega_A)^{-1}$ the two processes are decoupled yielding again a soft damping of the sound waves. Viceversa when $\tau_S \omega_A \sim 1$ the structural and acoustic phenomena have the maximum coupling yielding a maximum in the damping rate, see fig.5b). The dependence of ω_A on q produces a q -dependence of the coupling and also a departure $\Gamma_A \propto q^2$, as is seen clearly in fig.5. Γ_A at high temperature, far from the structural region, is not far from being proportional to q^2 . In the hypothesis of a single relaxation time we can extract its value from the damping maximum, i.e. $\tau_S \sim (\omega_A)^{-1}$. We found: $\tau_S \sim 0.6 \text{ nsec}$ for $q = 1 \text{ } \mu\text{m}^{-1}$, $\tau_S \sim 0.9 \text{ nsec}$ for $q = 0.63 \text{ } \mu\text{m}^{-1}$ and $\tau_S \sim 1.6 \text{ nsec}$ for $q = 0.338 \text{ } \mu\text{m}^{-1}$. This non negligible q -dependence of the structural relaxation time is again a mark of the inadequacy of the single time simple

analysis and/or a mark of the presence of heterogeneities.

When the temperature is around T_c , the structural relaxation process is appearing in the HD-TG pattern as a bump after the vanishing of the acoustic oscillations, see fig. 3. In that case the structural time can easily be extracted with confidence from the fitting procedure. Indeed only in a q -dependent restricted range of temperature it has been possible to get reliable structural parameters, τ_S and β , from our HD-TG data on OTP, namely in the range $T = 279 - 297 \text{ K}$ for $q = 1 \mu\text{m}^{-1}$, $T = 277 - 293 \text{ K}$ for $q = 0.63 \mu\text{m}^{-1}$ and $T = 272 - 287 \text{ K}$ for $q = 0.338 \mu\text{m}^{-1}$. This reflects the limitation of the fitting formulas, (eq.s 7, 11), since they fully applies only when a time scale separation exists among the various characteristic times, as already pointed out. Nevertheless these measurements are covering a key temperature range around the OTP critical temperature in a (q, t) or (q, ω) space quite difficult to reach by other techniques. The OTP structural parameters are reported in fig.6. They are covering three decades in time that was not previously investigated, from about 10 nsec up to $20 \mu\text{sec}$. Within the uncertainties resulting essentially from the fitting procedure, the structural relaxation times does not show any q -dependence and in the stretching parameter we cannot recognize any temperature dependent too. We want to remark that the stretching parameter is really affected by large uncertainties, see fig.6b). Unfortunately, also an other relevant quantity, i.e. the non-ergodicity parameter $f_{q \rightarrow 0}$ which can be estimated from eq. 10, is affected by large uncertainties. Within them, the $f_{q \rightarrow 0}$ parameter of OTP from our HD-TG data do not show the cusp-like behavior predicted by the mode-coupling theory [15], as is evident from fig.7. On the other hand, the behavior of the non-ergodicity parameter has been measured by neutron scattering for different high value of wave-vectors and by extrapolating its slope in the limit $q \rightarrow 0$ the cusp-like seem to be hardly visible [16].

The fit parameter τ_H , the thermal relaxation time, defines the final decay of the HD-TG signal and is safely extracted when the condition $\tau_H \gg \tau_S$ is verified. Since $\tau_H \sim 100 \mu\text{sec}$ and it is typically not strongly temperature dependent until T_g [7], it should be safely extracted in the range from 373 K down to 270 K . In figure 8 we report the thermal diffusivities,

$\chi = (\tau_H q^2)^{-1} = k(\rho_o C_p)^{-1}$, resulting from the investigated three wave-vectors in the whole temperature range. In the high temperature range χ shows the expected smooth variation and independence of q . Approaching the critical temperature, a strong deviation is showing up: starting from about 275 K at $q = 0.338 \mu m^{-1}$ (and from temperatures even higher at higher q) an anomalous strong decrease in the thermal diffusivity is coming from our fit. The decrease is so strong that the longer decay is clearly visible if we plot the data in a semilogarithmic scale, as in fig.9. This effect could be an interaction between the structural and thermal relaxation time constant, τ_S and τ_H , that are getting closer decreasing the temperature. However, when the thermal diffusivity starts to deviate, the structural and thermal relaxation times seem to be too far each other, e.g. at $q = 0.338 \mu m^{-1}$ the deviation start at about $T = 275 K$, where $\tau_S = 15 \mu s$ and $\tau_H = 115 \mu s$. Anyway we want to remember that τ_S is a parameter of a time distribution rather than the real relaxation time. Further, in the region of the thermal diffusivity dip, the HD-TG data show at long times a second very slow decay: indeed it is clear from fig.9, that the slow relaxation at $T = 283 K$ and $253 K$ are characterized by a single exponential relaxation, the thermal decay, and viceversa at $267 K$ some extra relaxation is appearing. It is fairly obvious that the used response function (eq.s 7, 11) is not able at all to reproduce these features. As regards the subsequent large increase of the thermal diffusivity at low temperature where the structural relaxation times are found even longer than the thermal relaxation, the experiments of specific heat spectroscopy on glass-formers [17] suggest that the increase can be due to C_p approaching the solid-like or high frequency response.

VI. DISCUSSION AND CONCLUSIONS

The present analysis in terms of density hydrodynamics response of the HD-TG data of glass-forming OTP around the critical temperature of the structural arrest, shows some clear results but also open some problems in the data interpretation. To get a further understanding, we compare our parameters with the other data from literature. In fig.10

we report our sound velocities together with the data from Brilluoin LS [18] and ultrasound experiments [19]. Here the agreement is very nice. As expected, there is a clear dispersion effect in q , as the LS data are taken at much higher wave-vectors, and the extreme values c_0 and c_∞ are approached at high and low temperatures respectively. It is evident that the HD-TG experiment is able to measure the sound velocity at wave-vectors in an otherwise difficult range, too low for LS techniques but too high for ultrasound experiments. In fact, in our experiment ω_A ranges from 0.4 to 2 *GHz* with $\Gamma_A \sim 2 - 160$ *MHz*.

Our structural relaxation times are compared with the light scattering (LS) [20,21], photon correlation (PC) [20,22] and time-resolved optical Kerr effect (OKE) data [23]. All these data are extracted from experiments performed with depolarized light geometry and so the influence of the orientational dynamics can be non negligible. Nevertheless, our OTP data, spanning from 10^{-8} up to 10^{-5} sec, nicely cover the gap present between LS, OKE and PC measurements and they follow the same course, as we can see in fig. 11. This good agreement has some implication in OTP dynamics suggesting that the orientational and translational dynamics have substantially the same temperature dependence, in the investigated temperature range, with very similar relaxation times.

The cusp-like behavior of the Debye-Waller factor expected in the frame of mode-coupling theory for a fragile glass such as OTP, is not recognizable, owing to large uncertainties.

We would like to stress that the slow thermal decay, at relatively low temperature, did not show a simple single exponential decay and can not be properly characterized by the simple hydrodynamics model used in this work. We have found this behavior common to other several glass-formers: glycerol, *m*-toluidine, salol [24]. In our opinion the apparent modification of the thermal diffusivity has to be addressed to effects of the structural dynamics on the thermalization process. In other word, the heat flux, produced by the weak absorption of the pump laser pulses, modify the kinetic energy of the different degree of freedom and not all of them thermalize in a very short time scale. Furthermore part of the roto-translational energy thermalizes through collective rearrangements that act on the structural time scale. This kind of processes are also responsible of the frequency dependence of

the specific heat. A more suitable hydrodynamic treatment for the heat transport should be able to taken into account the complex relaxation patterns found in the present experiment.

ACKNOWLEDGMENTS

We thank F.Barocchi, K.A.Nelson, R.M.Pick and G.Ruocco for very helpful suggestions and discussions. This work was supported by the Commission of the European Communities through the contract No HPRI-CT1999-00111, by MURST and by INFN through the project TREB-Sez.C-PAISS1999.

REFERENCES

- [1] J.Wong and C.A.Angell, *Glass structure by spectroscopy* (Marcel Dekker Inc., New York, 1976) P.G.Debenedetti, *Metastable Liquids* (American Chemical Society, Washington, 1996); J.T.Fourkas, D.Kivelson, U.Mohanty, and K.A.Nelson, *Supercooled Liquids* (Princeton University Press, New Jersey, 1996).
- [2] W.Götze, J.Phys.: Condens. Matter, **11**, A1 (1999); H.Z. Cummins, J.Phys.: Condens. Matter, **11**, A95 (1999).
- [3] R.Torre, P.Bartolini, R.M.Pick, Phys. Rev. E **57**, 1912 (1998), R.Torre, P.Bartolini, M.Ricci R.M.Pick, Europhysics Letters. **52**, 324 (2000), G.Hinze, D.D.Brace, S.D.Gottke, and M.D.Fayer, Phys.Rev.Lett. **84**, 2437 (2000).
- [4] A.Taschin, R.Torre, M.Ricci, M.Sampoli, and C.Dreyfus, R.Pick, /cond-matter/0106632.
- [5] G.Hinze, R.S.Francis, and M.D.Fayer, J. Chem. Phys. **88**, 6477 (1999).
- [6] H.J.Eichler, P.Gunter, and D.W. Pohl, *Laser-Induced Dynamic Gratings* (Springer-Verlag, Berlin, 1986).
- [7] Y.Yang and K.A.Nelson, **74**, 4883, Phys.Rev.Lett.(1995), Y.Yang and K.A.Nelson, **103**, 7732, J.Chem.Phys. (1995), and D.M.Paolucci and K.A.Nelson, **112**, 6725, J.Chem.Phys. (2000).
- [8] Y.Yan and K.A.Nelson, **87**, 6240, J. Chem. Phys.(1987); *ibid*: page 6257.
- [9] A.A.Maznev, K.A.Nelson and J.A.Rogers, **23**, 1319, Opt. Lett. (1998).
- [10] G.D.Goodno, G.Dadusc and R.J.Dwayne Miller, **15**, 1791, J.Opt. Soc. Am. B (1998).
- [11] B.B.Berne and R.Pecora, *Dynamic Light Scattering* (Wiley, New York, 1976).
- [12] J.P.Boon and S.Yip, *Molecular Hydrodynamics* (McGraw-Hill, New York, 1980).

[13] Y.Yang and K.A.Nelson, J.Chem.Phys. **103**, 7722 (1995).

[14] According to the hydrodynamics model [7] the whole ISBS signal is the following:

$$G_{\rho\rho}(q, t) \simeq C [e^{-\Gamma_A t} \sin(\omega_A t)] + D [-e^{-\Gamma_A t} \cos(\omega_A t) + e^{-(t/\tau_S)^\beta}]$$

Indeed the amplitude D has been found in the previous work to be negligible. Also in the present work we found the D terms to be very small and not affecting at all the fitting results Nevertheless, since this test is based only on the fitting procedure not a final conclusion can be given about the intensity of structural contribution in the ISBS signal.

[15] W.Götze and L.Sjögren, Rep. Prog. Phys. **55**, 241 (1992).

[16] A.Tölle, H.Schober, J.Wuttke and F.Fujara, Phys. Rev. E **56**, 809 (1997); E.Bartsch, F.Fujara, B.Geil, M.Kiebel, W.Petry, W.Schnauss, H.Sillescu and J.Wuttke, Physica A **201**, 223 (1993).

[17] N.O.Birge, Phys.Rev. B **34**, 1631 (1986).

[18] G.Monaco, D.Fioretto, L.Comez, G.Ruocco, Phys. Rev. E **63**, 61502 (2001).

[19] G. D'Arrigo, J. Chem. Phys. **63**, 61 (1975).

[20] W.Steffen, A.Patkowski, G.Meier and E.W.Fisher, J.Chem.Phys. **96**, 4171 (1992); W.Steffen, A.Patkowski, H.Glaser, G.Meier and E.W.Fisher, Phys.Rev.E **49**, 2992 (1994); A.Patkowski, E.W.Fisher, W.Steffen, H.Glaser, M. Baumann, T.Ruths and G.Meier, Phys. Rev. E **63**, 61503 (2001).

[21] H.Z.Cummins, G.Li, W.Du, Y.H.Hwang and G.Q.Shen, Prog.Theor.Phys.Suppl. **126**, 21 (1997).

[22] Y.H.Hwang and G.Q.Shen, J.Phys.C **11**, 1453 (1999).

[23] S.D.Gottke, D.D.Brace, G.Hinze and M.D.Fayer, J. Phys. Chem. B **105**, 238 (2001).

[24] M.Sampoli et al., in preparation; R.DiLeonardo et al., in preparation.

TABLES

T (K)	$q = 0.338 \mu m^{-1}$		$q = 0.630 \mu m^{-1}$		$q = 1.00 \mu m^{-1}$		$\frac{\Delta\omega_A}{\omega_A}$	$\frac{\Delta\Gamma_A}{\Gamma_A}$
	ω_A (GHz)	Γ_A (MHz)	ω_A (GHz)	Γ_A (MHz)	ω_A (GHz)	Γ_A (MHz)		
243.2	—	—	1.572	3.30	—	—	$\leq 0.1 \%$	$\leq 1 \%$
244	0.8348	2.94	—	—	—	—	"	"
253.2	—	—	1.525	3.81	2.423	6.47	"	"
254	0.8094	3.02	—	—	—	—	"	"
263.2	—	—	1.474	6.90	2.343	8.57	"	"
264	0.7821	3.52	—	—	—	—	"	"
270	0.7629	4.53	—	—	—	—	"	"
271.2	—	—	1.424	8.90	2.273	12.7	"	"
279.2	0.7275	10.1	1.381	15.2	2.195	22.3	"	"
287.2	0.693	22.1	1.319	35	2.10	45	$\leq 0.5 \%$	$\leq 5 \%$
295.2	0.642	44	1.240	68	2.00	86	"	"
303.2	—	—	1.139	93	1.868	142	"	"
304	0.577	50	—	—	—	—	"	"
313.2	—	—	1.025	86	1.674	156	"	"
314	0.52283	30	—	—	—	—	"	"
323.2	—	—	0.948	41	1.539	95	$\leq 0.1 \%$	$\leq 1 \%$
324	0.4977	11.9	—	—	—	—	"	"
333.2	—	—	0.913	20.8	1.462	52.7	"	"
334	0.4837	5.96	—	—	—	—	"	"
343.2	—	—	0.888	12.8	1.415	31.5	"	"
344	0.4715	3.87	—	—	—	—	"	"
353.2	—	—	0.866	9.37	1.377	21.8	"	"
354	0.4600	2.93	—	—	—	—	"	"
363.2	—	—	0.8441	7.34	1.342	15.8	"	"
364	0.4485	2.47	—	—	—	—	"	"
373.2	—	—	0.8236	6.38	1.309	12.8	"	"
374	0.4375	2.23	—	—	—	—	"	"

TABLE I. Sound frequencies and damping rates with their relative errors for the analysed q -values in the range 243 - 374. To avoid overcrowded table we report only some temperatures. K.

FIGURES

FIG. 1. Optical set-up and laser system for HD-TG experiment with optical heterodyne detection: M: mirror; CL#: cylindrical lens; DM: dichroic mirror; DOE: diffractive optic element; AL#: achromatic lens; APD: avalanche photodiode.

FIG. 2. Typical HD-TG raw data corresponding to phase difference between signal and local reference of $\Delta\varphi = 0^\circ$ and $\Delta\varphi = 180^\circ$ (above); pure HD-TG signal (below) is obtained by subtracting the two previous signals. The subtraction permits to improve substantially the signal/noise ratio and to remove the homodyne and all spurious contributions that are phase independent.

FIG. 3. HD-TG data on OTP for two wave-vectors, $q = 0.338$ and $q = 1 \mu m^{-1}$, at several temperatures. The data, at all temperatures, show damped acoustic oscillations at short times and thermal diffusion at long times. Decreasing of temperature the structural relaxation mode, typical of complex liquids, appears at first as strong acoustic damping ($\omega_A\tau_S \sim 1$ condition) and later as gradual rise of TG signal.

FIG. 4. HD-TG data (solid lines), fits (dotted lines) and residues $\times 3$ (lower lines) for OTP, at the two temperatures, $T = 288K$ and $T = 267K$ at wave-vector $q = 0.338 \mu m^{-1}$.

FIG. 5. Sound velocities C_A (a) and acoustic damping rates Γ_A (b) versus temperature from fits to HD-TG data at the investigated wave-vectors. At each q -value the sound dispersion and damping rate reach the maximum at the temperature at which $\omega_A\tau_S \sim 1$.

FIG. 6. Structural relaxation times τ_S and stretching parameter β versus temperature at the three wave-vectors analysed.

FIG. 7. Temperature dependence of the Debye-Waller factor, $f_{q \rightarrow 0}(T)$, in OTP, obtained by fits, at all wave-vectors. There is no evidence of a MCT cusp in the analysed temperature range .

FIG. 8. Thermal diffusivity versus temperature. For every investigated q -value, the extracted thermal diffusivity show, at low temperatures, a peculiar behavior not in agreement with the temperature dependence of the thermodynamic thermal diffusivity.

FIG. 9. HD-TG data (solid curves) and fits (dotted curves), at wave-vector $q = 0.338 \mu m^{-1}$ at some temperatures, are plotted in log-lin scale to show the complex decay at long times. In the intermediate temperatures range, where the thermal diffusivity (fig. 8) shows the anomalous dip, the used fitting function (11), is not able to reproduce the tail at long times.

FIG. 10. OTP sound velocities from HD-TG data, LS data [18] and ultrasonic measurements [19].

FIG. 11. OTP structural relaxation times from HD-TG data, LS [20,21], PC [20,22], and OKE data [23].

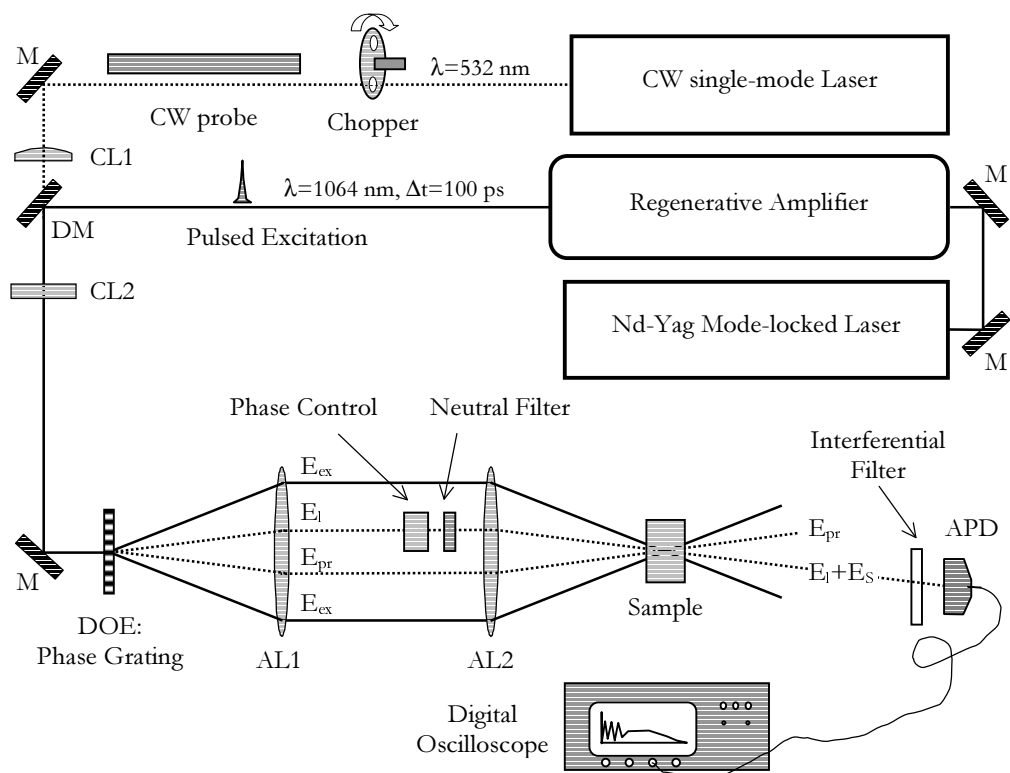


Figure 1

R. Torre et al.

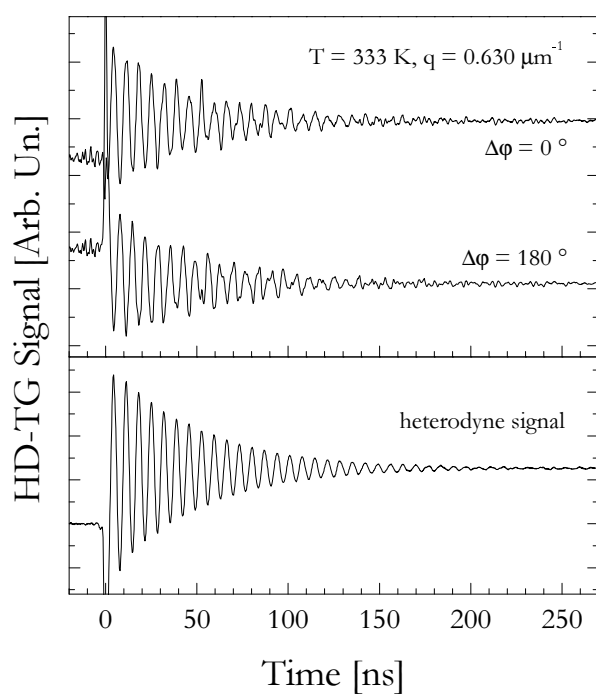


Figure 2

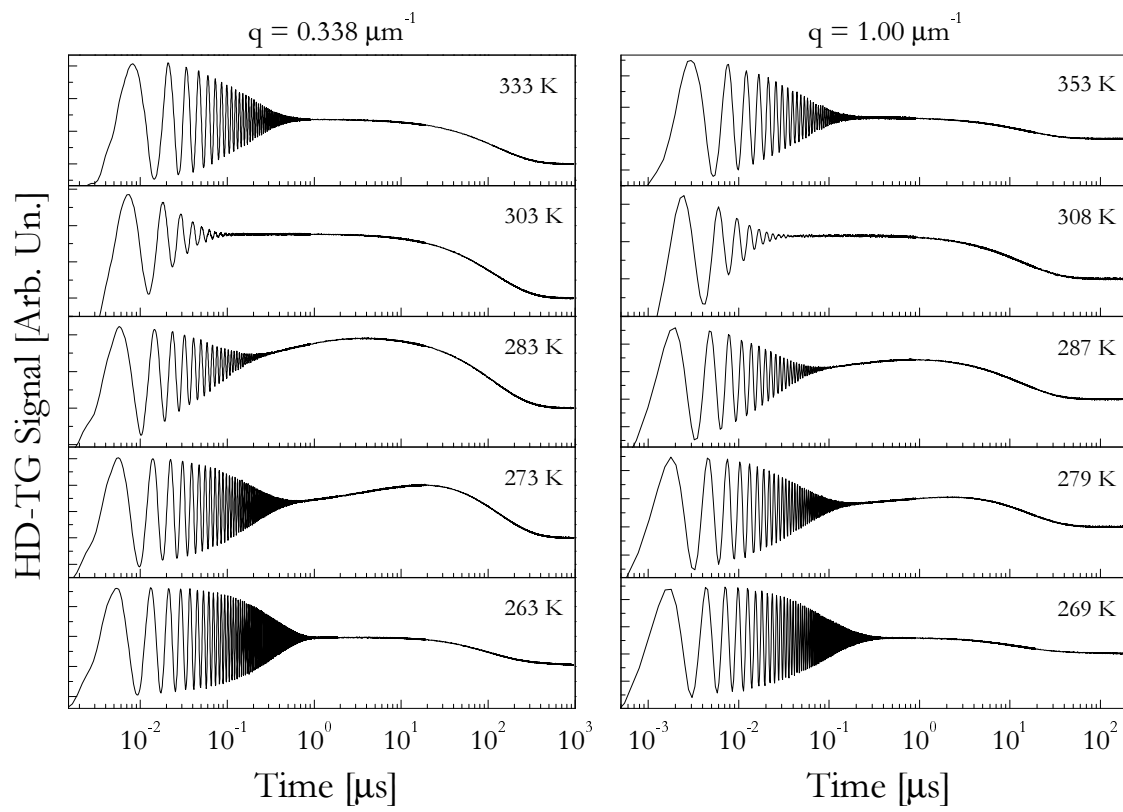


Figure 3

R. Torre et al.

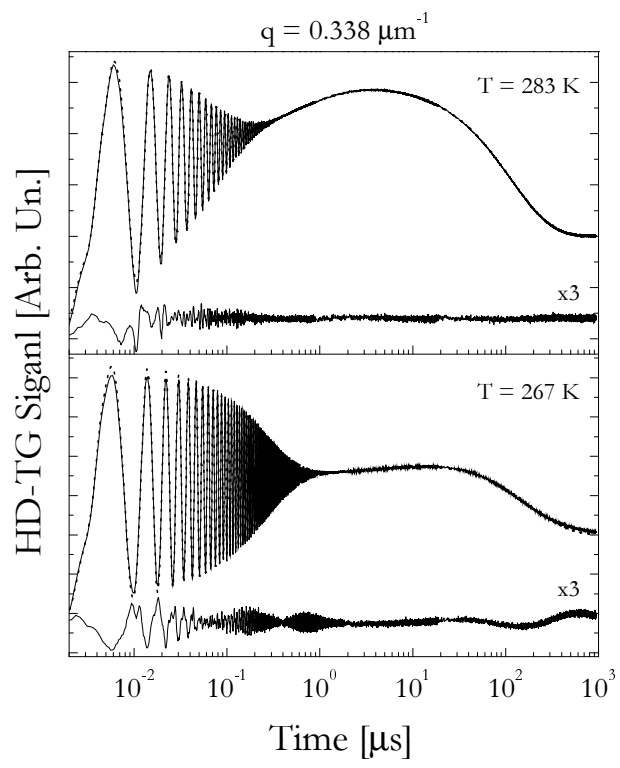


Figure 4

R. Torre et al.

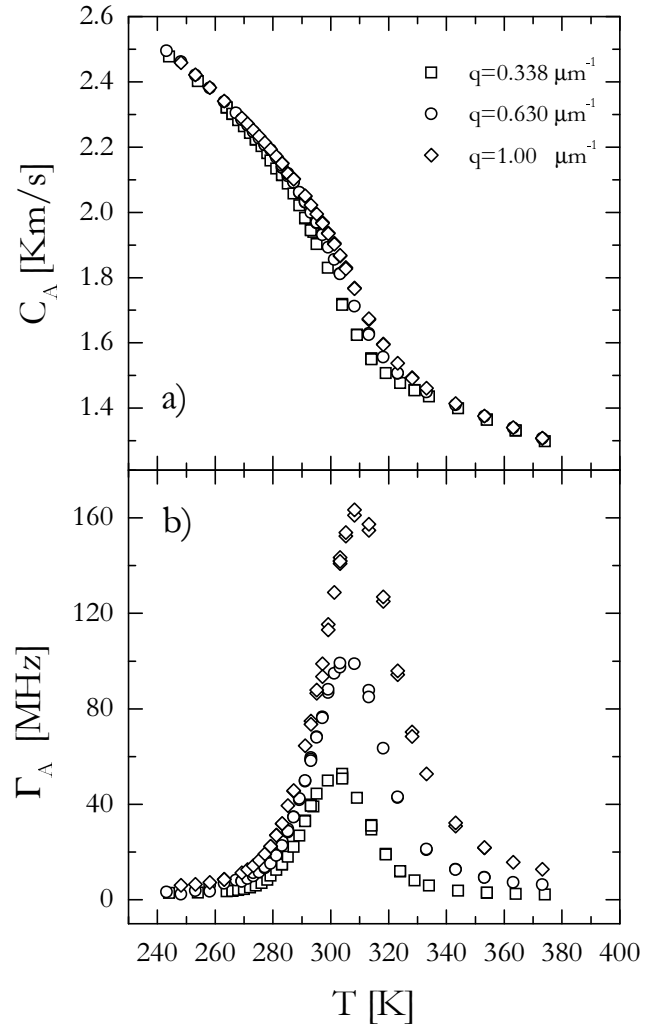


Figure 5

R. Torre et al.

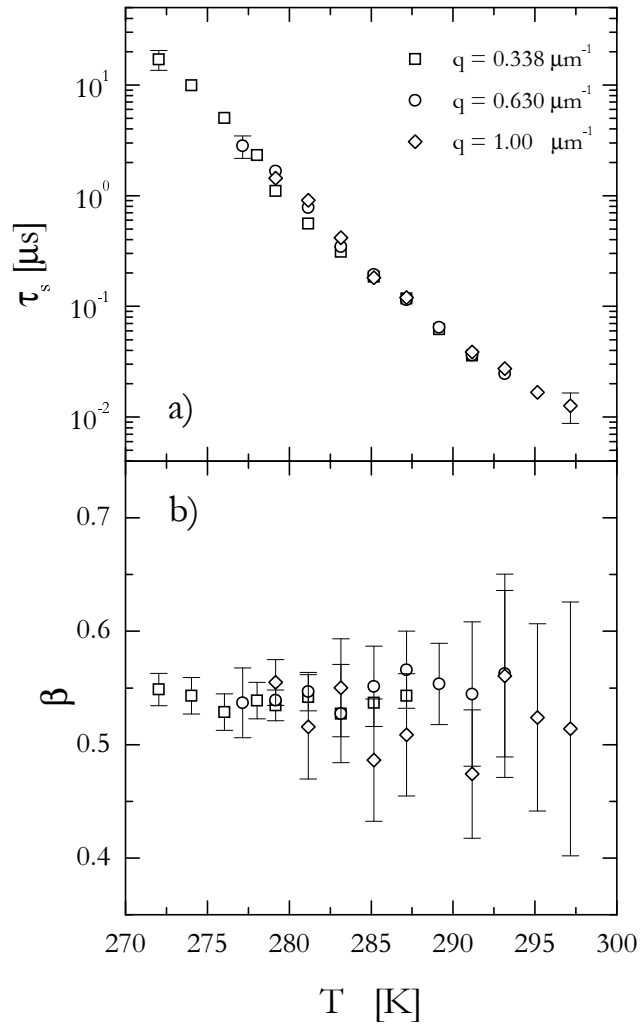


Figure 6

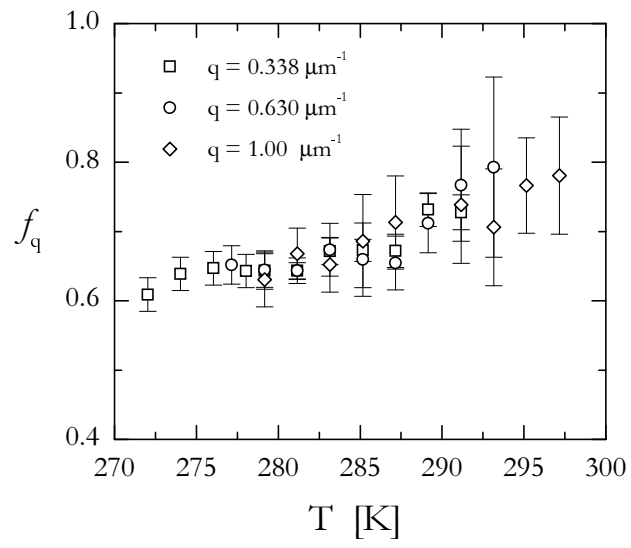


Figure 7

R. Torre et al.

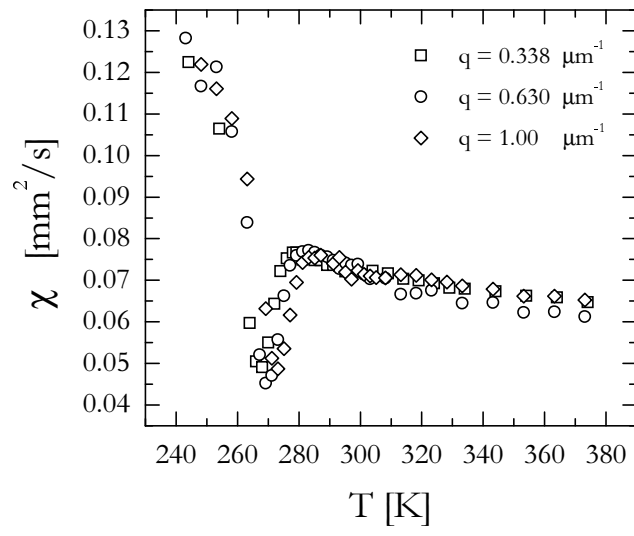


Figure 8

R. Torre et al.

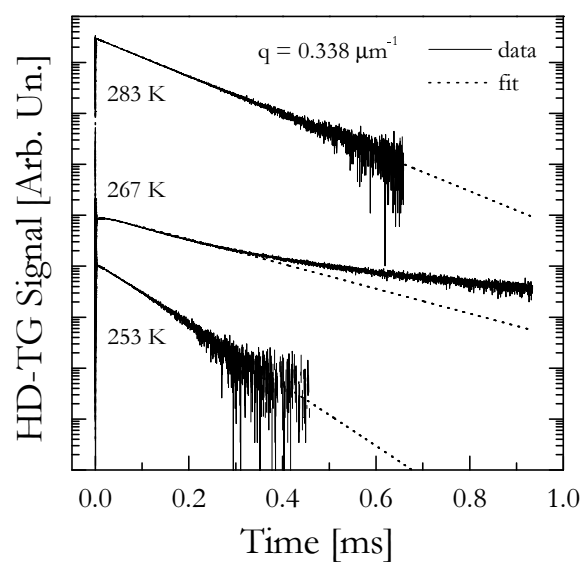


Figure 9

R. Torre et al.

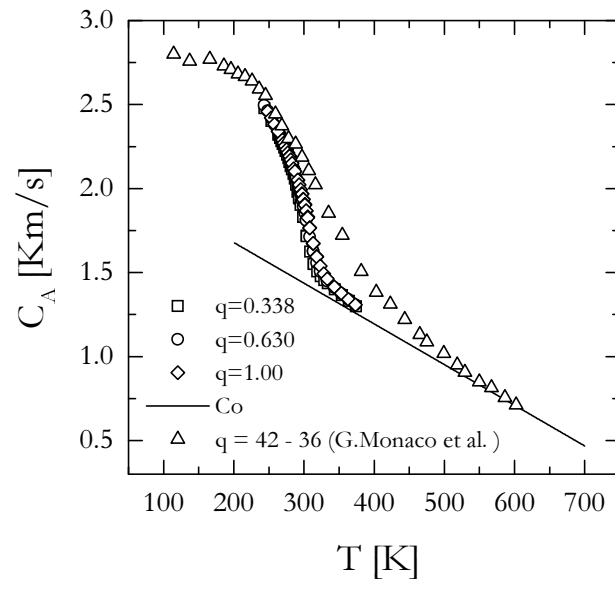


Figure 10

R. Torre et al.

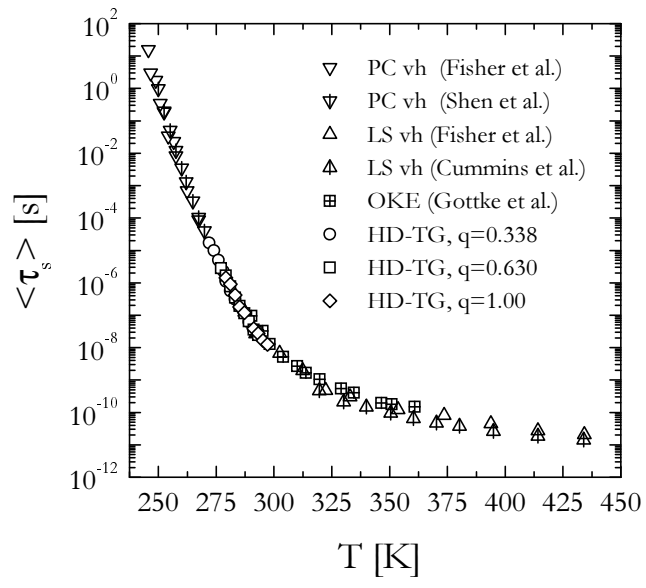


Figure 11

R. Torre et al.